Micro-analytical Technologies for Mineral Mapping and Trace Element Deportment

Ron F. Berry, Leonid V. Danyushevsky, Karsten Goemann, Anita Parbhakar-Fox and Thomas Rodemann

Abstract Quantifying the texture, mineralogy and mineral chemistry of rocks in the mine environment is required to predict the value of a deposit and maximize extraction efficiency. Scanning electron microscopy supported by recognition of minerals by characteristic X-ray emissions is the preferred mineral mapping method in the mining industry at present. This system is fully mature and supported by highly optimized software. Laser Raman mapping may compete for some of this space in the future. Very coarse scale mineral maps are possible from drill core images but these cannot be used to measure the key parameters required for most mine planning. Trace elements can be highly concentrated in rare minerals so that they are easy to detect but very difficult to accurately measure due to sampling problems, or they may be very dispersed and difficult to detect at all. There are a range of tools available to support trace element deportment and most studies will need to use more than one methodology. The key new development of the last decade is the emergence of laser ablation inductively coupled plasma mass spectrometry for the measurement of most elements at sub-ppm level. There are still many trace and minor elements for which accurate models of deportment are extremely difficult.

R.F. Berry (✉) · L.V. Danyushevsky · A. Parbhakar-Fox
School of Physical Sciences, University of Tasmania, Private Bag 79,
Hobart, TAS 7001, Australia
e-mail: Ron.Berry@utas.edu.au

L.V. Danyushevsky
e-mail: l.dan@utas.edu.au

A. Parbhakar-Fox
e-mail: Anita.Parbhakar@utas.edu.au

K. Goemann · T. Rodemann
Central Science Laboratory, University of Tasmania, Private Bag 74,
Hobart, TAS 7001, Australia
e-mail: Karsten.Goemann@utas.edu.au

T. Rodemann
e-mail: Thomas.Rodemann@utas.edu.au

B. Lottermoser (ed.), *Environmental Indicators in Metal Mining*,
DOI 10.1007/978-3-319-42731-7_4

Introduction

Quantifying the texture, mineralogy and mineral chemistry of rocks in the mine environment contributes to the prediction of three components of mine planning: processing performance, value of mine products and the environmental cost of the project. The element deportment explains the grade and recovery of mine concentrates. The value of the concentrate is also affected by the presence of penalty elements. For example in iron ore, Al and P are significant penalty elements. In base metal concentrates typical penalty elements are Sb, As, F and Hg. The number of penalty elements in smelting is increasing and the grade at which they apply is decreasing as environmental monitoring at the smelting site becomes more stringent.

For environmental assessment of mining we need to focus on the characterization of mine waste and prediction of mineral and element behaviour in the environment. This is a complex area (Smith and Huyck 1999; Plumlee 1999). There are environmental challenges associated with all the mine waste streams: process water, mine water, mine waste, dust and tailings. The environmental impact of these streams is strongly affected by the mineralogy and trace element composition of both the ore and waste components of the mine.

This chapter concentrates on how mineral mapping and trace element methods can contribute to a discussion of the methods and impacts of mining. It is restricted to methods that are employed by industry and researchers now, or which are on the fringe of economic application. The methodologies include conventional mineral mapping techniques (optical microscopy, SEM/EDS, infrared) and emerging technologies (Laser Raman, X-ray CT). In trace element mapping the conventional scanning electron microscope (SEM) based energy dispersive spectroscopy (EDS) and wavelength dispersive spectroscopy (WDS) element mapping is compared with micro-X-ray fluorescence, micro-proton-induced X-ray emission (PIXE), and laser ablation inductively coupled plasma mass spectrometer (LA-ICPMS). More sophisticated analytical tools such as X-ray absorption near-edge spectroscopy (XANES), synchrotron-based microanalysis and surface techniques (e.g. X ray photoelectron spectroscopy) are not included. The aim is to promote a better understanding of how mineralogical information is collected and used for problem solving in the mining industry.

Mineral Mapping

Mineral mapping is carried out at a range of scales. There is a constant tension between the need to get high precision results on a sample and the extent to which the samples measured are representative of the material that will be processed. In the past, studies have failed to properly represent the spatial variability of the orebody. A relatively small number of samples have been well characterized. Sampling statistics were carefully monitored to make sure the sample sent for measurement

was properly represented but very little attention was paid to whether this sample was representative of the ore and waste that may be produced across the life of the mine.

More recently, this problem has been realized and attempts have been made to use less precise but cheaper tests to define the variability before large scale sampling is carried out for robust testing. This problem has not yet been solved. Mineralogy tests are available for major minerals but textural attribute and trace mineral abundance measurements are very expensive to carry out in the numbers required to define the ore body variability.

Petrology and many geology studies are based on intact textures. They provide a first look at the material but cannot provide the statistical support needed for rigorous predictions of mine performance. Representivity requires that tests are carried out on particles. Most authors (e.g. Geelhoed 2011) suggest that for particulate material a reasonable sampling error is achieved where 1000s of particles are measured, and more are required where a trace element, such as Au, is concentrated in a trace mineral.

When measuring grain size and shape parameters, it is important not to modify the grain size in the sample preparation. The usual recommendation is to have a particle size at least five times the largest grain size to be measured. For example, in liberation prediction it is important to recognise grains coarser than the mill grind size. Putting these two requirements together means that the particle size studied must be greater than 0.5 mm (cf. $\sim$1 mm of Sutherland 2007). In a sample sieved to +0.6−1.2 mm, a typical grain mount has 200–500 particles. Berry and Hunt (2011) suggest that the error on the P50 grain size estimate for chalcopyrite was about 10 % relative in a low grade Cu deposit using a single grain mount.

Mineral mapping is expensive and should be used with care. The experimental design should include a clear statement of what data is required that can only be generated from mineral maps. Grain size distribution can be the rate controlling factor for reactions in the environment but often modal mineralogy is more important. Bulk methods for mineralogy have significant advantages over mineral maps in estimating modal mineralogy. For accurate mineral mapping the scanning electron microscope remains the method of choice but for the spatial variation of the deposit a cheaper protocol is required and in some circumstance optical microscopy or even classification of drill core images may be useful.

Automated Optical Microscopy

Generation of mineral maps by optical methods has a long history, but early attempts were limited by the lack of digital images and computing capacity. Modern optical analysis of mineral textures was summarized by Higgins (2006). Automated recognition has largely been applied to opaque minerals (e.g. Pirard 2004; Pirard et al. 2007; Lane et al. 2008). However, transparent mineral can be analysed using object-oriented multi-spectral methods (Berry et al. 2008).

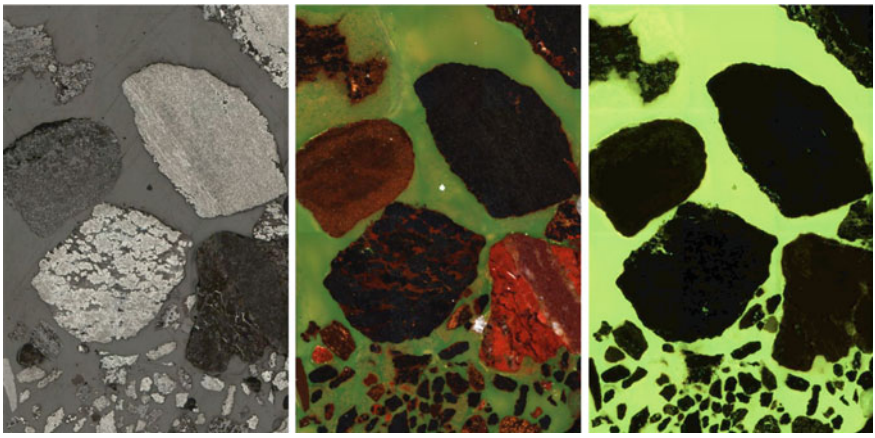

Fig. 1 Grain mount of iron ore as polished block. *Left* reflected light, *Middle* reflected light cross polarized, *Right* fluorescent image (field of view 1.5 mm wide) (color figure online)

Automated optical mineral identification requires a microscope with a high precision stage (position reproducibility better than 1 micron) that allows direct tiling of frames and good registration of multiple images. For large scale imaging a 5× objective lens gives 10 μm resolution. This provides the best balance between resolution, depth of focus and field of view. For best results great care is required with colour balance and shading correction. Multiple transmitted and reflected light images are required for accurate classification. For particle mounts a fluorescence dye can be added to the resin to aid recognition of particle boundaries (Fig. 1). Classification accuracy varies from 85 to 95 % in simple systems with less than eight significant minerals. Trace mineral recognition is not recommended unless the mineral has outstanding optical properties.

The optical mineral mapping protocol occupies a discrete niche in the environmental geometallurgy toolset. In a few cases such as separating hematite from magnetite and marcasite from pyrite, optical microscopy is better than SEM-EDS mapping, which could prove particularly useful in acid rock drainage (ARD) prediction studies. Where only the opaque minerals need to be identified then optical microscopy can be effective. If the aim is the recognition of both transparent and opaque minerals, and especially if there are less than ten minerals involved, then object-oriented multi-spectral software provides an efficient environment for the development of the complex rules base required.

SEM-EDS Mapping

Scanning electron microscopes (SEM) with fast energy dispersive X-ray detectors (EDS) are currently the method or choice for mineral mapping in the minerals

industry (e.g. Goodall and Scales 2007). The SEM has a high resolution with an excellent depth of field, so it is easy to map quickly at a large range of magnifications while the sample stays in focus. The usual sample is a grain mount (particles) with a polished surface coated with carbon. The main limit to mapping resolution is the interaction volume between the electron beam and the sample. For a typical 15–25 keV electron beam this is up to 5 µm diameter and 5 µm deep. For higher resolution a lower accelerating voltage is required but can make recognition of the minerals using characteristic X-rays more difficult as the K· X-ray lines of many elements are not activated at this electron energy. At 7 keV the interaction volume is 0.3–0.5 µm across, depending on mineral density and mean atomic number.

The standard image on a SEM is the secondary electron (SE) image. The SE image is based on low energy electrons that are the result of inelastic scattering. SE images predominantly show topography which is of little use in mineral mapping. However, it can be useful in recognising if bacterial catalysis of ARD has taken place, with pits seen on pyrite mineral surfaces, or to observe morphological changes during ARD evolution (e.g., Weber et al. 2004). An alternative image available on most SEMs is the back scattered electron (BSE) image which is strongly controlled by the sample mean atomic number (Howell et al. 1998). This image has lower sensitivity to surface imperfections and topography, but a high quality final polish of the sample surface (e.g. 0.25 micron diamond) are still required to prevent topographical information masking compositional variations. It provides a robust basis for mineral mapping (Fig. 2). The BSE image is based on high energy primary electrons re-emerging from the sample surface with some of their energy left. Its application in environmental characterization studies is well documented (e.g., Weisener and Weber 2010; Smart et al. 2010).

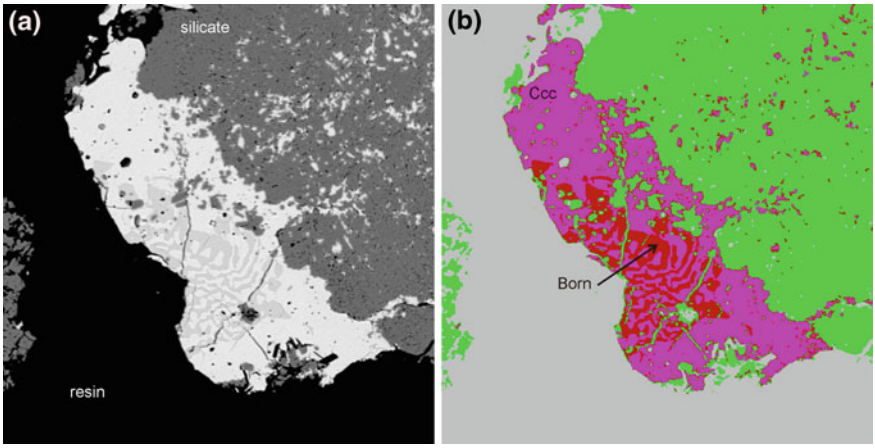

Fig. 2 **a** BSE map of vermicular bornite in chalcocite. **b** Classification of sulfides (Ccc-chalcocite, Born-bornite) based on BSE intensity (color figure online)

Major advances in beam current and detectors have led to substantial improvements in SEM-EDS mapping over the last 20 years. There are two commonly used software solutions for mineral mapping:

(a) Collect an X-ray spectra at every pixel (Gottlieb et al. 2000), or
(b) Use a BSE map to recognize objects and then collect the X-ray spectra from each object (Gu 2003; Fandrich et al. 2007).

The former method is more robust but the second is quicker. All SEM-EDS methods require a mineral spectra library to undertake the classification step, i.e. matching a spectrum obtained from an X-ray analysis of the unknown to one stored in the mineral spectra library. The library is key resource that has to be established for each project. While library spectra can be collected with moderate count times, during the analysis the count time for each spectrum is a key decision which defines the speed and accuracy of the analysis.

Laser Raman Spectroscopy

Raman scattering is the inelastic scattering of photons. When photons are scattered from an atom or molecule, most photons are elastically scattered (Rayleigh scattering). About 1 in 10 million photons are scattered by an excitation, with the scattered photons having an energy different from the incident photons by the energy level of one of the electrons involved in chemical bonding in the material. These differences are the same as the absorption energies in infrared spectroscopy but are measured as a difference from the incident laser light energy rather than at a fixed wavelength. Thus electron energy differences that would normally be far into the infrared can be moved to the visible light range and the spatial resolution of laser Raman analysis defined by the spot size of the laser beam rather than the optical resolution of infrared light. The Raman effect differs from the process of fluorescence. In fluorescence, the incident light is completely absorbed and the fluorescence photon is emitted after a resonance lifetime. Fluorescent light is a feature of the material and does not change with the laser frequency.

Laser Raman spectroscopy is a rapidly developing field in mineralogy. Raman spectroscopy is used to identify a wide variety of minerals and, in some instances, to provide chemical and structural information (Das and Henry 2011). It is useful for mineral identification across the whole range of minerals: silicates, oxides and sulfides. It has spatial resolution down to 1 μm. However, historically, this technology was too slow for routine mapping functions. Recently, a new generation of fast-mapping laser Raman spectrometers have been released with mapping rates of 50 ms/pixel. This rate is similar to the SEM-EDS mapping systems 15 years ago, when the first SEM-EDS software was evolving. A modern Raman instrument is a desktop machine based around a conventional optical microscope. Raman

spectroscopy is a low-cost, rapid, high-resolution technique which requires minimal sample preparation and is well suited to mine waste recognition (Levitan et al. 2009; Stefaniak et al. 2009; Das and Henry 2011).

Polymorphs such as pyrite and marcasite have the same chemical formula and identical composition. They cannot be differentiated by normal SEM-EDS mapping. However, marcasite is more reactive than pyrite and the proportion of marcasite is significant in mineral processing and environmental impact of mining. The Raman spectrum of marcasite is different from pyrite (Hope et al. 2001).

The presence of carbonaceous material is important in predicting leach extraction behaviour (Helm et al. 2009) and fO_2 buffering potential of mine waste. Carbonaceous material is easily recognized by Raman spectroscopy (Wopenka and Pasteris 1993) but not by SEM-EDS mapping. Mapping of carbonaceous material is feasible (Fig. 3), but care must be taken in selection of laser frequency to avoid fluorescence.

Raman spectroscopy is increasingly being used in the analysis of oxidized waste materials. It can be used to identify a wide range of environmentally sensitive minerals such as arsenates (Filippi et al. 2007, 2009). It also has potential application to the recognition of dust mineralogy (e.g. Huang et al. 2013) but few examples are publicly available.

X-Ray CT

X-ray computed tomography (X-ray CT) was initially implemented in the medical field, and is an emerging technology in mineral mapping (Kyle and Ketcham 2015). The technology is developing dramatically from a purely research interest 10 years ago to active application in porosity mapping (Knackstedt et al. 2009) and diamond search (Firsching et al. 2012) today. Gold deportment is likely to be the next widespread commercial implementation in the minerals industry (Dominy et al. 2011).

X-ray CT depends on the attenuation (absorption) of X-rays by materials. At low to medium energies (up to 100 keV) X-rays are largely attenuated by photoelectric absorption. This process is controlled by electron density which is a monotonic function of atomic number. Each element has additional capacity to absorb above specific energies associated with the characteristic absorption edges for that element. For common elements in the Earth these absorption edges are less than 10 keV, but high atomic number elements have higher energy absorption edges (e.g. K absorption edge for Au is 81 keV, and for U is 115 keV). At higher energies, the predominant effect is Compton scattering, which is less dependent on atomic number (Fig. 4). As a result, compositional differences have a greater impact on X-ray CT contrast at lower energies, whereas contrast at higher energies is linearly dependent on differences in density. To image materials that differ in composition (elemental) but not mass density, X-rays <100 keV are used. Diamond search uses this difference (Basis Material Decomposition: BMD) to identify the high density but low atomic number diamonds (Firsching et al. 2012). No

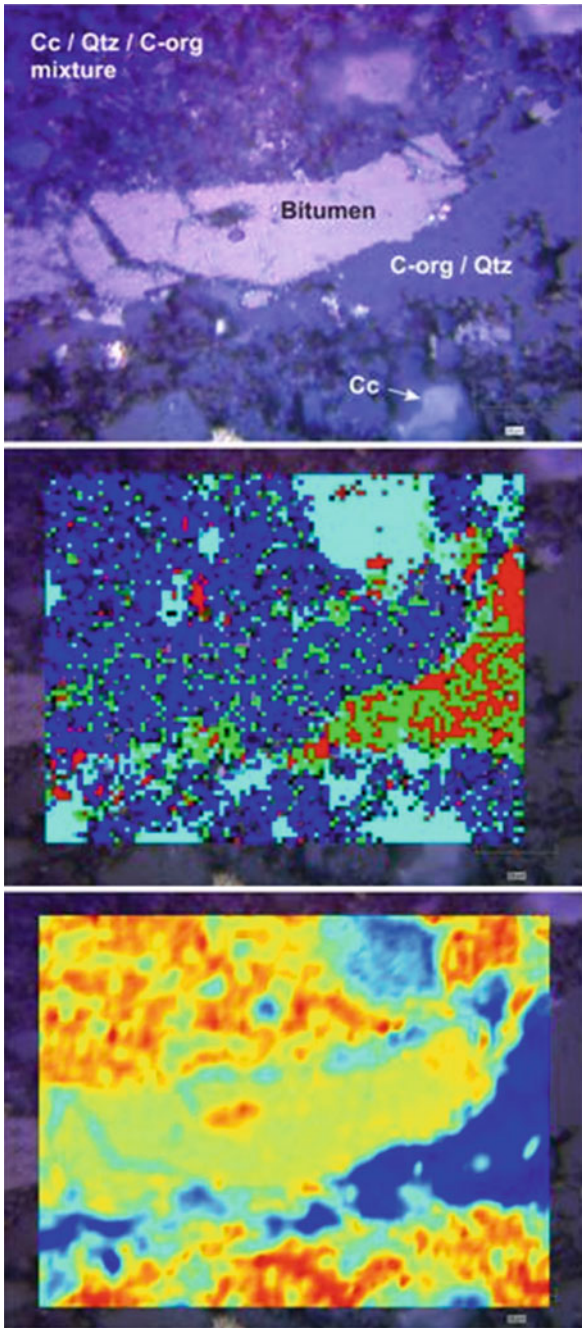

Fig. 3 *Top* reflected light image; *Middle* hierarchical cluster analysis for all components recognized. Colours for clusters: *blue* Carbon, *green* quartz, *red* sulfide (possibly marcasite), *cyan* calcite. *Bottom* heat (warm colours) map shows the probability the pixel is mostly graphite. Note, the central bitumen region shows lower intensity than true graphite which reflects the different spectra of organic C. *Cc* calcite, *qtz* quartz, *C-org* carbonaceous material (color figure online)

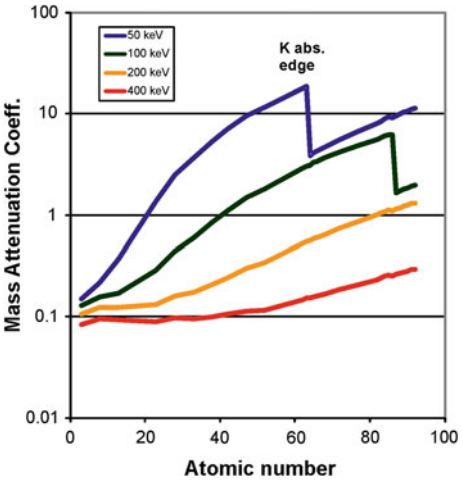

Fig. 4 X-ray mass attenuation coefficient (cm^2/g) across atomic number range for four X-ray energies (based on data in Hubbell and Seltzer 1996) (color figure online)

application of this technique for the development of environmental indicators has been found to date.

Core Imaging

Visible Light

High quality core photographs are technically feasible. A pixel size of 100 μm (250 dpi) gives excellent quality and allows for recognition of grains larger than 0.5 mm. This resolution is not sufficient to determine grain size distribution in most ores. Theoretical optical resolution limits should allow a higher resolution to be achieved but experiments suggest little extra information is obtained because of the surface roughness.

Lighting is of prime importance to producing a high quality photographic record of the core. All the evidence suggests that the core must be kept wet to give good results. With wet core, specular reflection from the water surface is common and the lights must be placed to avoid this problem.

For a photographic record that enhances direct comparison of core intervals it is important that lighting is stable over the life of the project. The protocol must include a colour balance check every day. A light intensity standard should be recorded on a daily basis so any drift in conditions can be corrected. A shading correction is essential if mineral maps are to be produced. In saturated pixels all colour information is lost. If mineral maps are to be produced, the brightness should be adjusted to avoid saturated pixels.

Low quality mineral maps can be produced from core images (Fig. 5). A few minerals can be conclusively identified but most of the core is classified into

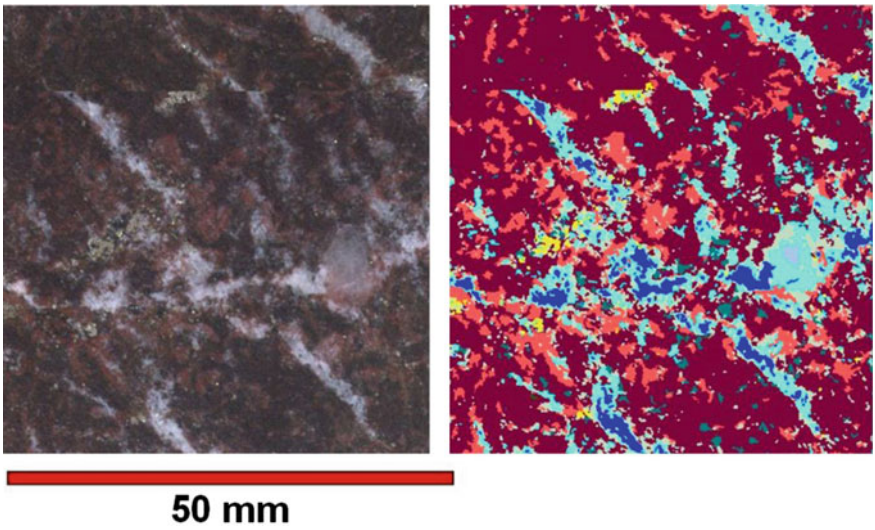

Fig. 5 High quality core image from cut core (*left*) and the derived mineral map (*right*) including coarse grained chalcopyrite (*yellow*) (color figure online)

mineral associations. This is most effective where the ore is coarse grained and minerals have a high visual contrast. These maps provide a textural basis for classification. They are not competitive with other methods where the main aim is determining the mineralogy of core intervals.

Infrared Mapping

A recent advance has been the development of "high" resolution infrared mapping devices suitable for core. Core scanning devices can measure maps in near infrared (NIR) and short wave infra-red (SWIR) bands at 0.5 mm pixels. These devices are excellent for mapping the distribution of IR active minerals such as hydrous silicates and carbonates. The spatial resolution means they cannot be used to recognize mineral grains or even grain aggregates except in the coarsest grained rocks. Thermal infrared (TIR) maps which include a wider range of minerals are now possible but have poor spatial resolution.

The infrared core scanning devices typically have optional high resolution visible light photography but the IR imperative is that core is completely dry so the visible light images lack the clarity that might otherwise be expected.

Core scale mineral mapping using IR hyperspectral mapping is limited by its spatial resolution. This emerging technology is yet to find its correct niche in environmental geometallurgy.

Trace Element Deportment

All the problems of sampling support and representivity discussed for mineral mapping also affect trace element deportment. The most extreme sampling problems are for trace elements that are concentrated at high level in trace minerals. For this case, sampling errors dominate over all other sources of error. This topic has received extensive study for precious metals (e.g. Smee and Stanley 2005) but not for other trace elements.

The first indication for trace element deportment can be found in element correlation tables based on whole rock geochemistry. This information can save a lot of effort by targeting the initial search at specific minerals. Based on that data the methods can be selected from those below. It is very difficult to determine the distribution of 100 % of a trace element. Commonly only 75 % of the trace element assay is accounted for in deportment studies.

Electron Probe Micro Analysis (EPMA)

The classical method for measuring trace and minor elements in minerals is electron probe micro analysis (EPMA). This is a SEM-based method with an electron beam hitting the target and producing characteristic X-rays which are measured with wavelength dispersive spectrometers (WDS) or with solid state crystals that can determine the energy of the individual X-rays (EDS). For EPMA, a specialized SEM is used that has an optical microscope to set the specimen position and is designed for high regulated beam currents. Major developments have been in the new electron sources, LaB_6 crystal and field emission (FE), which provide a much smaller spot size where the electron beam hits the sample.

The WDS are much more expensive, include many high precision moving parts, have very high spectral resolution ($\sim$5 eV) and measure characteristic wavelengths sequentially. A full feature EPMA system has five WDS so that five elements can be measured at once. Modern developments are low noise gas flow detectors, large area analysing crystals and high speed counting electronics. In typical spot mode WDS methods have a detection limit of 50–300 ppm (e.g. F: 200 ppm, Si, Fe: 60 ppm, Co, Ni: 100 ppm, Cu, Zn: 130 ppm, As: 170 ppm, Se, Ag: 200 ppm, Au, Hg, Pb, Bi: 300 ppm). Under optimum circumstance in research condition some elements can be detected below 10 ppm (Wark and Watson 2006). In mapping mode the detection limit is much higher.

EDS are cheaper with no moving parts, have lower spectral resolution (120–140 eV at Mn Kα peak) and measure all wavelengths at once. The low spectral resolution means that the continuous X-rays provide a higher background against which to measure the characteristic X-rays and as a result the detection limit for most elements is much higher. This is especially true when measuring L X-ray lines (elements with atomic number >30). In addition overlap between characteristic X-ray

lines is much more common for L and M X-ray lines. The EDS detectors have improved in the last 15 years with liquid N_2 free detectors, better spectral resolution, larger area detectors and especially higher effective count rates. The computing power has greatly improved the background estimation and full peak series deconvolution of these devices is now standard (Ritchie et al. 2012). In normal circumstances, in spot mode, a detection limit of 0.1 % is an achievable and in optimal circumstances detection limits of 200 ppm have been reported (Donovan 2011).

The normal mode of operation for EPMA is spot analysis. Up to 20 elements are analysed using a 1–10 μm spot (5–14 μm diameter analysed area) in 2 to 5 min. Major elements take 20–40 s, five elements at a time. Errors are 3–5 % relative for elements >500 ppm. Spots can be pre-programmed individually, in scan lines or over a grid. A few hundred analyses can run unattended overnight. Acquisition conditions for X-ray element mapping depend on the elements being measured (X-ray energies to be excited) and the stability of mineral(s) being mapped. For silicates and carbonates, 15 keV accelerating voltage and 100 nA beam current are typically used. For sulfides, 20 keV and 100–300 nA are commonly used. Maps range from 512 * 384 pixels to 4096 * 4096 pixels (Fig. 6). Pixel sizes are usually 1–20 μm. Five WDS X-ray lines are measured in each scan. Major elements can be measured using EDS at the same time. Maps are usually accumulated at 10–100 ms/pixel. At 100 ms/pixel (detection limit around 1000 ppm), it takes 450 h to complete a single pass of 4096 * 4096 pixels, so trace element mapping is usually done over small areas or at low resolution. A more realistic scan time is 11 h with a 2048 * 2048 pixel area and 10 ms/pixel ($\sim$3000 ppm detection limit). For lower detection limits other techniques such as LAM-ICP-MS are preferred.

The electron microprobe analyser has an important role in measuring trace element abundances in the range 200–5000 ppm using spot mode. Trace element maps can be generated in WDS mode for elements where the important

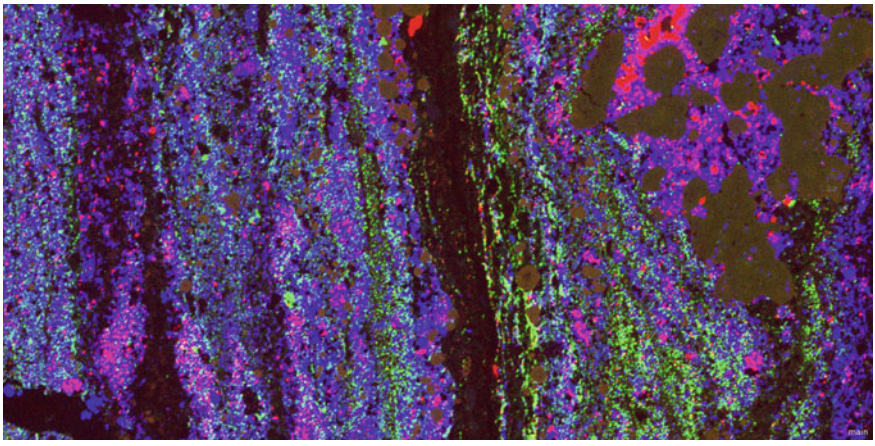

Fig. 6 EPMA map of fine grain massive sulfide ore. 1536 * 768 pixels at 1 μm/pixel. Cu in *red*, Pb in *green* and Zn in *blue* (color figure online)

compositional range is above 1000 ppm. Most elements above atomic number 4 can be measured but for routine application the element range is F to U (atomic number 9–92). It is suitable for most elements of interest in environmental impact assessments such as As, Bi, Cd, Ni and F. EDS detectors on modern SEMs, especially with FE electron sources, will measure the same elements with a detection level 3× to 5× higher.

Micro XRF

In the last 10 years it has been possible to routinely focus X-rays onto a spot as small as 10 μm. The X-rays are generated by a standard X-ray tube and focused through a mono- or poly-capillary optic. When high energy X-rays hit a target they generate characteristic X-rays from the target (at energies much less than the source beam). The advantage of using an X-ray source to generate X-ray fluorescence (XRF) is that there is a much lower background of continuous X-rays so detection limits are lower, the sample does not need to be coated, and the measurement can be carried out in air if only high atomic number elements are to be measured. The disadvantages are that X-rays are hard to focus so intensities are low, XRF is not effective for light elements (below Na), and the primary X-ray beam has very high penetration so the analysis is an integration of the composition down to 100s of microns depth for more energetic characteristic X-rays. At small spot sizes, up to 100 μm, the X-ray intensity of the primary beam is low so that analysis is slow.

Our experiments with micro XRF suggest it has limited application in environmental indicators. It may be suitable for mapping of delicate materials (unsuitable for a vacuum), where the very long count times needed for realistic detection limits have to be accepted because no other technique can be applied. A new generation of micro XRF is now appearing which may overcome some of the problems experienced.

Laser ICP-MS

The laser ablation inductively coupled plasma mass spectrometer (LA-ICP-MS) combines three specific elements. The sample is usually mounted in a resin block (25 mm diameter) and placed in a sample chamber below the laser. The sample chamber is flushed with Ar gas. Helium gas is bled in through an internal small sample enclosure. The laser beam is turned on and ablates the surface. Fine particles are carried by the He and then Ar gases through a set of plastic mixing tubes to the plasma. At the plasma the particles are vaporized and ionized before introduction into a fast switching quadruple mass spectrometer which measures various atomic weight ions.

LA-ICP-MS is an in situ technique with moderate spatial resolution. Sample preparation is relatively simple requiring a moderately polished surface and no

coating. The major advantage of this technique is the very low detection limit for most elements. There are substantial consumable costs, mainly for inert gases He and Ar, which limit application in mapping to specific high value areas. There are a range of interferences from charged oxides and argides, which make some elements difficult to measure in a typical rock matrix. In addition, the results are sensitive to machine drift which can affect absolute abundance measurements. Laser ablation rates are matrix sensitive so that the mineral must be known before the raw counts can be converted to element abundance.

The major application for LA-ICP-MS is to provide rapid trace element analytical capabilities with a typical detection limit of 0.1–20 ppm. It is possible to detect some heavy elements at ppb level. In analytical mode the typical analysis time is about 90 s.

In mapping mode the sample is rastered under the laser beam in a series of closely-spaced lines. The ablated material takes several seconds to reach the mass spectrometer so a correction must be made for this delay. To minimize the delay a small volume ablation cell is required. Good quality maps (Fig. 7) require long term laser stability. Typically a first run is made to pre-ablate the sample to remove surface contamination of trace elements. Map quantification has low precision and spot measurements are made after the map has been compiled to get absolute abundances of the elements in the zones that are distinguished.

LA-ICP-MS mapping has lower spatial resolution than SEM-based mapping, and is 10 to 100 times slower. It is also destructive with 5 µm of material ablated from the surface during mapping. LA-ICP-MS mapping has detection limits from 100 to 1000 times lower than SEM-WDS maps. The main application of this technique is in mapping trace elements such as Au, As and Bi to determine the possible path of these elements in the mineral processing system.

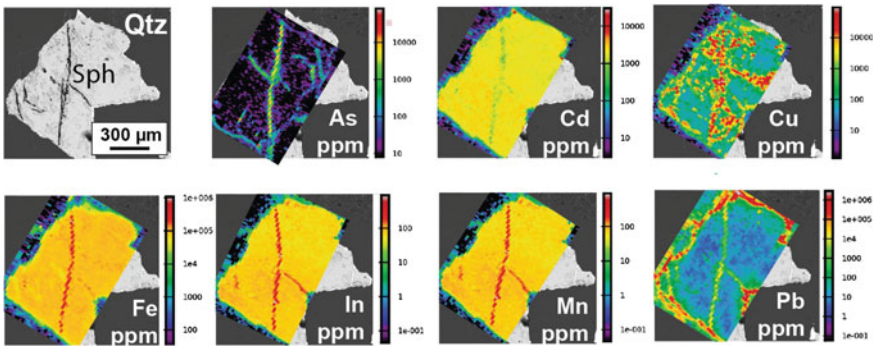

Fig. 7 Maps showing the distribution of seven trace elements in a grain of sphalerite (BSE map at *top left*). Sample after 10 weeks of leaching in a kinetic test. As concentrated in fractures. Pb concentrated in fractures and around the grain. Fe, In and Mn still homogeneously distributed and showing no evidence of leaching (color figure online)

Other Techniques

Just as an electron beam can generate characteristic X-rays in EPMA, a high energy proton beam will generate characteristic X-rays when it hits a solid target (Ryan 2000). This is the basic concept of PIXE (proton-induced X-ray emission analysis). The proton beam is accelerated to very high energy (>1000 keV), which gives a high ratio of characteristic X-ray emission to the continuous X-ray spectrum (bremsstrahlung). The lower background leads to lower detection limits. The typical PIXE machine uses an EDS detector so the detection limit is still more than 1 ppm. The spot size can be as small as 1 micron but resolution is affected by spreading and depth penetration of the beam just as with the SEM. The high energy proton beam has much higher depth penetration (several tens of microns) than typical electron beams and this means the depth resolution is less than the lateral variation on the maps. For imaging, the proton beam is rastered across the surface just as with small area EPMA maps. However, at this time the PIXE appears to be limited to research only applications by cost and availability.

Where sub-micron resolution trace and minor element mapping is required, ion beams (charged atoms) can be used to splutter material from the surface of a specimen that is then transferred into a mass spectrometer for measurement. This is known as secondary ion mass spectrometry (SIMS). The most common secondary ion used is mass filtered oxygen ($16O^-$) with Cs^+ used where a positive ion is required. Typical applications map at 10 μm pixel resolution and measure isotopes and trace elements (down to sub ppm concentration levels). SIMS analysis for sub-microscopic gold in sulfides is commercially available. It has a much smaller spot size than LA-ICP-MS and a higher detection limit (250 ppb). Because of speed (cost) considerations it is losing market share to LA-ICP-MS in trace element mapping. The cost and time preclude the widespread use of SIMS in the minerals industry, with applications limited to specific highly targeted solutions.

Conclusions

There are many ways to map mineral distributions. The optimum method depends on the aim.

(a) Where 3D connectivity is a key theme, as in porosity mapping, the X-ray CT systems are rapidly improving and already look competitive for specific problems.
(b) For high resolution mineral maps in complex systems (multi-mineral, fine grain size) the SEM-EDS mapping systems are the best today. The laser Raman mapping systems may be competitive in this field within a few years.
(c) For a simple system (e.g. iron ore) or where only a few minerals need to be mapped the automated optical microscope may be a cost competitive system. The optical method cannot compete in sparse phase search with the SEM-EDS

mapping. It does have advantages of the SEM-EDS system in a few specific problems such as mapping assemblages that contain polymorphic minerals (e.g. marcasite and pyrite).

(d) Mapping the surface of rough samples is available via laser Raman spectroscopy and while slow at the moment may be routine within 2 years. The confocal capacity of these systems also allows maps below the surface where minerals are transparent to the laser light.

(e) PIXE has significant advantages for mapping the chemistry of objects below the surface.

The SEM-EDS mapping systems dominate mineral mapping at present. They are highly optimized with efficient commercial software support. Competing systems will find it difficult to change this within the next 5 years. In that period, the alternative methods are likely to encroach as niche methods in specific problems that lend them an advantage.

Trace element deportment is a complex problem. Before starting the search for trace element sources in a specific project it is essential to consider the options. When attempting to find trace elements to define the deportment there are several possible scenarios:

- Trace element is concentrated as a major (stoichiometric) element in a trace mineral: Sparse phase SEM-EDS mapping to recognize all relevant trace minerals. Examples are: Au in gold and electrum; F in fluorite; As in arsenopyrite, cobaltite, realgar, orpiment and enargite; Bi in Bi metal, bismuthinite and some sulfosalts; Cd in greenockite; Pb in galena and some sulfosalts; Sb in stibnite and some sulfosalts; Ni in Ni sulfides; U in uraninite, coffinite and carnotite.
- Trace element is concentrated as a minor element in a minor mineral: SEM-EDS point counting to recognize all relevant minor minerals. EPMA or EDS to measure minor element abundance in mapped minerals. Examples are: F in apatite, mica, amphibole, tourmaline; As in pyrite and low-As sulfosalts; Cd in sphalerite; Pb in low Pb sulfosalts; Ni in pyrite, olivine, mafic minerals, clays; U in apatite, zircon, allanite, monazite, REE phosphates.
- Trace element is dispersed at trace level in a common mineral: SEM-EDS point counting or QXRD to measure abundance of common mineral. LA-ICP-MS to measure trace element content of the host minerals. Examples are: Au in pyrite and arsenopyrite; Bi in pyrite; Cd in pyrite; Pb in feldspar; Sb in pyrite; U in feldspar.

In many cases, the element of interest may be found in more than one of these scenarios. In all cases, some combination of techniques will probably be required to find the location of most of a trace element in a sample. The big change in trace element deportment studies over the last few years has been the emergence of the LA-ICP-MS as an efficient high throughput device with sub-ppm detection limits for most elements.

References

Berry RF, Hunt J (2011) Grain size in geometallurgy: review of progress. Geometallurgical mapping and mine modelling (AMIRA P843A). Technical Report 8, pp 61–75, Nov 2011

Berry RF, Walters SG, McMahon C (2008) Automated mineral identification by optical microscopy. In: Ninth International Congress for Applied Mineralogy, Brisbane, pp 91–94

Das S, Henry MJ (2011) Application of Raman spectroscopy to identify iron minerals commonly found in mine wastes. Chem Geol 290:101–108

Dominy SC, Platten IM, Howard LE, Elangovan P, Armstrong R, Minnitt RCA, Abel RL (2011) Characterisation of gold ores by X-ray computed tomography—part 2: applications to the determination of gold particle size and distribution. In: Dominy SC (ed) First AusIMM international geometallurgy conference (GeoMet) 2011, pp 293–309

Donovan JJ (2011) High sensitivity EPMA: past, present and future. Microsc Microanal 17:560–561

Fandrich R, Gu Y, Burrows D, Moeller K (2007) Modern SEM-based mineral liberation analysis. Int J Mineral Process 84:310–320

Filippi M, Doušová B, Machovič V (2007) Arsenic in contaminated soils and anthropogenic deposits at the Mokrsko, Roudný, and Kašperské Hory gold deposits, Bohemian Massif CZ. Geoderma 139:154–170

Filippi M, Machovič V, Drahota P, Böhmová V (2009) Raman micro-spectroscopy as a valuable additional method to XRD and EMPA in study of iron arsenates in environmental samples. Appl Spectroscop 63:621–626

Firsching M, Nachtrab F, Mühlbauer J, Uhlmann N (2012) Detection of enclosed diamonds using dual energy X-ray imaging. In: 18th World conference on nondestructive testing, 16–20 April 2012, Durban, South Africa, pp 1–7

Geelhoed B (2011) Is Gy's formula for the fundamental sampling error accurate? Experimental evidence. Min Eng 24:169–173

Goodall WR, Scales PJ (2007) An overview of the advantages and disadvantages of the determination of gold mineralogy by automated mineralogy. Min Eng 20:506–517

Gottlieb P, Wilkie G, Sutherland D, Ho-Tun E, Suthers S, Perera K, Jenkins B, Spencer S, Butcher A, Rayner J (2000) Using quantitative electron microscopy for process mineralogy applications. JOM 52:24–25

Gu Y (2003) Automated scanning electron microscope based mineral liberation analysis. J Min Mat Charact Eng 2:33–41

Helm M, Vaughan J, Staunton WP, Avraamides J (2009) An investigation of the carbonaceous component of preg-robbing gold ores. World gold conference 2009, The Southern African Institute of Mining and Metallurgy, 2009

Higgins MD (2006) Quantitative textural measurements in igneous and metamorphic petrology. Cambridge University Press, Cambridge

Hope GA, Woods R, Munce CG (2001) Raman microprobe mineral identification. Min Eng 14:1565–1577

Howell PGY, Davy KMW, Boyde A (1998) Mean atomic number and backscattered electron coefficient: calculations for some materials with low mean atomic number. Scanning 20:35–40

Huang Q, McConnell LL, Razote E, Schmidt WF, Vinyard BT, Torrents A, Hapeman CJ, Maghirang R, Trabue SL, Prueger J, Ro KS (2013) Utilizing single particle Raman microscopy as a non-destructive method to identify sources of PM10 from cattle feedlot operations. Atmos Environ 66:17–24

Hubbell JH, Seltzer SM (1996) Tables of X-ray mass attenuation coefficients and mass energy-absorption coefficients from 1 keV to 20 MeV for elements Z = 1 to 92 and 48 additional substances of dosimetric interest. NIST. http://www.nist.gov/pml/data/xraycoef/index.cfm/

Knackstedt MA, Latham S, Madadi M, Sheppard A, Varslot T, Arns C (2009) Digital rock physics: 3D imaging of core material and correlations to acoustic and flow properties. Lead Edge 28:28–33

Kyle JR, Ketcham RA (2015) Application of high resolution X-ray computed tomography to mineral deposit origin, evaluation, and processing. Ore Geol Rev 65:821–839

Lane GR, Martin C, Pirard E (2008) Techniques and applications for predictive metallurgy and ore characterization using optical image analysis. Min Eng 21:568–577

Levitan D, Hammarstrom JM, Gunter ME, Seal RR, Choul IM, Piatek N (2009) Mineralogy of mine waste at the Vermont asbestos group mine, Belvidere Mountain, Vermont. Am Miner 94:1063–1066

Pirard E (2004) Multispectral imaging of ore minerals in optical microscopy. Min Mag 68:323–333

Pirard E, Lebichot S, Kreir W (2007) Particle texture analysis using polarized light imaging and grey level intercepts. Int J Miner Process 84:299–309

Plumlee GS (1999) The environmental geology of mineral deposits. In: Plumlee GS, Logsdon MJ (eds) The environmental geochemistry of mineral deposits part A: processes, techniques and health issues. Rev Econ Geol 6A:71–116

Ritchie NWM, Newbery DE, Davis JM (2012) EDS measurements of X-ray intensity at WDS precision and accuracy using a silicon drift detector. Micros Microanal 18:892–904

Ryan CG (2000) Quantitative trace element imaging using PIXE and the nuclear microprobe. Int J Imag Sys Technol 11:219–230

Smart RStC, Miller SD, Stewart WS, Rusdinar Y, Schumann RE, Kawashima N, Li J (2010) In situ calcite formation in limestone-saturated water leaching of acid rock waste. Sci Total Environ 408: 3392–3402

Smee BW, Stanley CR (2005) Sample preparation of 'nuggety' samples: dispelling some myths about sample size and sampling errors. Explore 126:21–26

Smith KS, Huyck HLO (1999) An overview of the abundance, relative mobility, bioavailability, and human toxicity of metals. In: Plumlee GS, Logsdon MJ (eds) The environmental geochemistry of mineral deposits part A: processes, techniques and health issues. Rev Econ Geol 6A:29–70

Stefaniak E, Alsecz A, Frost R, Mathe Z, Sajo IE, Torok S, Worobiec A, Griekent R (2009) Combined SEM/EDX and micro-Raman spectroscopy analysis of uranium minerals from a former uranium mine. J Hazard Mat 168:416–423

Sutherland D (2007) Estimation of mineral grain size using automated mineralogy. Min Eng 20:452–460

Wark DA, Watson BE (2006) TitaniQ: a titanium in quartz geothermometer. Contrib Mineral Petrol 152:743–754

Weber PA, Stewart WA, Skinner WM, Weisener CG, Thomas JE, Smart RStC (2004) Geochemical effects of oxidation products and framboidal pyrite oxidation in acid mine drainage prediction techniques. Appl Geochem 19: 1953–1974

Weisener CG, Weber PA (2010) Preferential oxidation of pyrite as a function of morphology and relict texture. NZ J Geol Geophys 53:22–33

Wopenka B, Pasteris JD (1993) Structural characterisation of kerogens to granulite-facies graphite: applicability of Raman microprobe spectroscopy. Am Miner 78:533–557